Atmos. Meas. Tech. Discuss., 6, 6517–6566, 2013
www.atmos-meas-tech-discuss.net/6/6517/2013/
doi:10.5194/amtd-6-6517-2013

Atmospheric Measurement Techniques Discussions
Open Access

Tropospheric CO vertical profiles deduced from total columns using data assimilation: methodology and validation

L. El Amraoui[1], J.-L. Attié[1,2], P. Ricaud[1], W. A. Lahoz[1,3], A. Piacentini[4], V.-H. Peuch[5], J. X. Warner[6], R. Abida[1], and J. Barré[7]

[1]CNRM-GAME, Météo-France and CNRS, UMR3589, Toulouse, France
[2]Laboratoire d'Aérologie, Université de Toulouse, CNRS/INSU, Toulouse, France
[3]NILU, 2027 Kjeller, Norway
[4]CERFACS, Toulouse, France
[5]ECMWF, Reading, UK
[6]Department of Atmospheric & Oceanic Science, University of Maryland, Baltimore County, USA
[7]NCAR, Boulder, USA

Received: 14 June 2013 – Accepted: 9 July 2013 – Published: 18 July 2013

Correspondence to: L. El Amraoui (laaziz.elamraoui@meteo.fr)

Published by Copernicus Publications on behalf of the European Geosciences Union.

Abstract

This paper presents a validation of a method to derive the vertical profile of carbon monoxide (CO) from its total column using data assimilation. The main motivation of this study is twofold. First, to deduce both the vertical CO profiles and the assimilated CO fields with good confidence. Second, for chemical species that can be measured only as the total column, this method provides an attractive alternative for estimating their vertical profiles in the troposphere.

We choose version 3 (V3) of MOPITT CO total columns to validate the proposed method. MOPITT has the advantage of providing both the vertical profiles and the total columns of CO. Furthermore, this version has been extensively validated by comparison with many independent datasets, and has been used in many scientific studies. The first step of the paper consists in the specification of the observation errors based on the Chi-square (χ^2) test. The observations have been binned according to day, night, land and sea (LAND_DAY, LAND_NIGHT and SEA, respectively). The respective optimal observation error values for which the χ^2 metric is the closest to 1 are: 7 %, 8 % and 11 % for SEA, LAND_DAY and LAND_NIGHT, respectively. In a second step, the CO total column, with its specified errors, is used within the assimilation system to estimate the vertical profiles. These are validated by comparison with vertical profiles of MOPITT V3 retrievals at global and regional scales. Generally, both datasets show similar patterns and good agreement at both global and regional scales. Nevertheless, the total column analyses (TOTCOL_ANALYSES) slightly overestimate CO concentrations compared to MOPITT observations. In a third step, vertical profiles calculated from TOTCOL_ANALYSES have been compared to those calculated from the assimilation of MOPITT V3 vertical profiles (PROFILE_ANALYSES). Both datasets shows very good agreement, but TOTCOL_ANALYSES tend to slightly overestimate CO concentrations. The mean bias between both datasets is 6 % and 8 % at the pressure levels 700 and 200 hPa, respectively. In terms of zonal means, the CO distribution is similar for both analyses. The mean bias between these datasets is low and doesn't exceed

AMTD
6, 6517–6566, 2013

CO total column assimilation

L. El Amraoui et al.

12 %. These results confirm that both analyses (total column and vertical profiles) are in very good agreement at global and regional scales.

1 Introduction

Carbon monoxide (CO) is an important atmospheric species as it influences tropospheric chemistry and climate (Crutzen and Andreae, 1990). The main sources of CO emissions are biomass burning, fossil fuel and the oxidation of methane and non-methane hydrocarbons (Granier et al., 2000). For this reason and because of larger anthropogenic emissions in the Northern Hemisphere (NH) than in the Southern Hemisphere (SH), tropospheric CO background are much higher in the NH than in the SH. The major global sink of CO in the troposphere is the chemical reaction with the hydroxyl radical (OH). Therefore, CO concentrations are higher in winter than summer owing to the seasonal variations of OH abundances. Since OH is the only significant tropospheric sink for CO and many other atmospheric trace gases emitted into the troposphere, CO has the potential to indirectly control the oxidation capacity of the troposphere. Therefore, an increase in CO emissions could reduce OH concentrations and, consequently, the oxidation capacity of the troposphere and its ability to remove pollutants (Mahieu et al., 1997).

Most of the CO in the troposphere is found in the lower troposphere or boundary layer. Compared to its inter-hemispheric mixing time of several years, CO is not well mixed in the free troposphere where it has a relatively long lifetime of several weeks to few months. This makes CO a useful tracer of air pollution, and allows studies of long-range transport of pollutants in the troposphere.

For more than 10 yr, global observations of tropospheric CO have been performed from several satellite instruments such as the Measurement of Air Pollution from Space (MAPS) onboard the Space Shuttle (Reichle et al., 1999), the Interferometric Monitor of Greenhouse Gases (IMG) onboard the ADEOS satellite (Clerbaux et al., 2001), the Measurement Of Pollution in the Troposphere (MOPITT) onboard Terra satellite (Drum-

AMTD
6, 6517–6566, 2013

mond and Mand, 1996), the SCanning Imaging Absorption spectroMeter for Atmospheric CHartographY (SCIAMACHY) onboard ENVISAT (Bovensmann et al., 1999), the Atmospheric Infrared Sounder (AIRS) onboard Aqua (McMillan et al., 2005) and the Tropospheric Emission Spectrometer (TES) onboard Aura satellite (Beer et al., 2001). All these measurements provide many opportunities to study tropospheric CO on a global scale. The Infrared Atmospheric Sounding Interferometer (IASI) onboard the MetOP-A (Meteorological Operational Program) satellite launched in October 2006 provides augmented horizontal resolution of the total column of many species such as ozone (O_3), nitrous oxide (N_2O), water vapour (H_2O), carbon dioxide (CO_2), chlorofluorocarbons (CFCs), methane (CH_4) and CO. Monitoring of these atmospheric species will continue with the METOP-B satellite which carries a suite of sophisticated instruments. These two satellites are polar orbiters and provide global observations. The data they collect on the atmosphere and the environment are complementary and allow the monitoring of the atmospheric composition and its evolution in near real-time.

Most tropospheric sensors operate with a nadir-viewing geometry and typically provide vertically integrated information, implying limited vertical resolution. This could present a limitation for some process studies such as long-range transport of pollutants because of missing information on vertical levels. Furthermore, most chemistry and transport models (CTMs) are subject to large uncertainties concerning the distribution of CO concentrations. This is because CO sources are not well known since their estimates are generally derived from inventory-based, bottom-up techniques which are highly uncertain (e.g., Jones et al., 2003). Another issue concerns the CO emissions from biomass burning which have unexpected sources in terms of time, location and magnitude and thus are subject to large uncertainties (Bian et al., 2007).

Chemical data assimilation consists of combining in an optimal way observations provided by instruments with a priori knowledge about a physical system such as model output. It allows constraints to be put on models using observations, and thus can be used to overcome model deficiencies. It also provides a four-dimensional (time and space) description of the dynamical and chemical state of the atmosphere. Typically,

AMTD
6, 6517–6566, 2013

data assimilation systems produce observation minus forecast (OMF) statistics that are used for monitoring biases between the observations and the models (e.g., El Amraoui et al., 2010). The specific objective of chemical data assimilation is to produce a self-consistent picture of the atmosphere taking into account both the available observations and our theoretical understanding of the atmospheric system.

Assimilation of CO satellite observations in the troposphere has been performed using different sensors. These include MAPS (Lamarque et al., 1999), IMG (Clerbaux et al., 2001), MOPITT (e.g. Pradier et al., 2006; Claeyman et al., 2010; El Amraoui et al., 2010) and SCIAMACHY (e.g. Tangborn et al., 2009). Most of the CO analyses in these studies have revealed improvements of the CO distribution in comparison to the free model run. However, no assessment of the impact of the assimilation of the total column on the CO vertical profile has been done hitherto.

The main goal of this study is to assess the benefit of the CO total column assimilation on the CO vertical distribution at global and regional scales. We choose Version 3 (V3) of MOPITT CO measurements to validate the proposed method. The motivation for this choice is presented in Sect. 2.1. The proposed method has the advantage of allowing fast computation of the vertical profiles and the analyses of CO. It will be particularly useful in the future when there will be many missions providing large volumes of data for which level 2 retrievals with their corresponding characteristics (covariance matrices and averaging kernels) will be very expensive in terms of computer resources (i.e., IASI onboard METOP-A and METOP-B or future geostationary missions). Furthermore, the assimilation of such data in CTMs taking into account all these characteristics will likely be very costly in terms of time computation and memory. This will be a significant shortcoming regarding the operational use of these data. Thus, the validation of the method proposed in this paper could be an alternative way to produce CO fields at global scale with relatively modest resources.

First, we describe the approach which consists of deducing the vertical distribution of CO in the troposphere from the assimilation of total column measurements (hereinafter noted TOTCOL_ANALYSES). Second, we validate the vertical profiles deduced

AMTD
6, 6517–6566, 2013

from TOTCOL_ANALYSES with the MOPITT retrieved vertical profiles. In a third step, we compare the vertical profiles deduced from TOTCOL_ANALYSES against those obtained from the assimilation of MOPITT CO vertical profiles taking into account the corresponding error covariance matrices and averaging kernels (hereinafter noted PROFILE_ANALYSES).

The paper outline is as follows: Sect. 2 presents the MOPITT CO measurements as well as the corresponding total columns, the data assimilation system used in this study, and the data used for the evaluation of the vertical profiles deduced from the assimilation of CO MOPITT total column: the official vertical profiles of MOPITT measurements. The method used for the assimilation of MOPITT CO total columns, the specification of the errors as well as the a posteriori diagnostics are presented in Sect. 3. The comparison of the vertical profiles deduced from CO TOTCOL_ANALYSES to those of MOPITT observations are presented in Sect. 4. Section 5 presents a validation of the vertical profiles calculated from CO TOTCOL_ANALYSES against the MOPITT PROFILE_ANALYSES. Conclusions are presented in Sect. 6.

2 Data and analysis

2.1 Terra/MOPITT carbon monoxide observations

The MOPITT instrument (Drummond and Mand, 1996) is onboard the Terra platform and has been monitoring global tropospheric CO from March 2000 to date. The pixel size is 22 km × 22 km and the vertical profiles for MOPITT version 3 (V3) are retrieved on 7 pressure levels (surface, 850, 700, 500, 350, 250 and 150 hPa) with the maximum likelihood method (Rodgers, 2000). The retrieved profiles are characterized by their error covariance matrices and their averaging kernels, providing information on the vertical sensitivity of the measurements. In particular, the Degrees of Freedom for Signal (DFS), the trace of the averaging kernel matrix, indicates the number of independent pieces of information in the measurements. It depends, via the surface temperature,

AMTD
6, 6517–6566, 2013

on latitude and time of day. The MOPITT V3 CO level 2 product consists of retrieved values and estimated uncertainties of the CO total column and CO profile (see: http://www.acd.ucar.edu/mopitt/retrievals.shtml). The retrieved CO total column is obtained as a byproduct of the retrieved profile by integrating the retrieved profile from the surface to the top of the atmosphere (see: www.acd.ucar.edu/mopitt/avg_krnls_app.pdf).

The main motivation for using the MOPITT V3 is because these data have been extensively validated against many independent datasets (e.g., Emmons et al., 2004, 2007, 2009; Deeter et al., 2007; Yurganov et al., 2008). The MOPITT V3 CO measurements are also well validated and have been used in many studies in relation with CO long-range transport (e.g., Heald et al., 2004); the influence of biomass burning on the distribution of O_3 in the lower troposphere (e.g., Zheng et al., 2004); the calculation of a CO surface source inventory (e.g., Heald et al., 2004; Pétron et al., 2004); North American pollution outflow (Li et al., 2005); and the temporal and spatial variability of CO (e.g., Bremer et al., 2004; Edwards et al., 2004). Note finally that the temporal and spatial behaviour of MOPITT V3 data is well understood. These data have also been extensively evaluated across a large range of spatial and temporal scales (e.g., Emmons et al., 2009).

The methodology developed in this paper consists of three steps. First, we deduce the vertical profiles from TOTCOL_ANALYSES. Second, the official vertical profiles of MOPITT V3 as delivered by the retrieval process are used to validate the vertical profiles deduced from the CO MOPITT V3 TOTCOL_ANALYSES. Third, we compare CO TOTCOL_ANALYSES for which the errors was specified based on the χ^2 test to those obtained from MOPITT V3 PROFILE_ANALYSES taking into account the corresponding error covariance matrices and averaging kernels. The objective of this last comparison is to evaluate the differences between both analyses (total column and vertical profiles).

AMTD
6, 6517–6566, 2013

2.2 MOCAGE CTM and data assimilation system

The assimilation system used in this study is MOCAGE-PALM (e.g., El Amraoui et al., 2008a) developed jointly by Météo-France and CERFACS (Centre Européen de Recherche et de Formation Avancée en Calcul Scientifique) in the framework of the ASSET (ASSimilation of Envisat daTa) European project (Lahoz et al., 2007). MOCAGE (MOdèle de Chimie Atmosphérique à Grande Echelle) (Peuch et al., December 1999) is a 3-D-CTM which covers the planetary boundary layer, the free troposphere, and the stratosphere. It provides a number of optional configurations with varying domain geometries and resolutions, as well as chemical and physical parameterization packages. It has the flexibility to use several chemical schemes for stratospheric and tropospheric studies. MOCAGE is used for several applications: operational chemical weather forecasting in Météo-France (Dufour et al., 2004); tropospheric and stratospheric research studies (e.g., Claeyman et al., 2010; Ricaud et al., 2009a,b); and data assimilation research (e.g., Semane et al., 2007, 2009; El Amraoui et al., 2008a; El Amraoui et al., 2008b, 2010; Claeyman et al., 2011b). In this study, MOCAGE is forced dynamically by wind and temperature fields from the ARPEGE model analyses, the global operational weather prediction model of Météo-France (Courtier et al., 1991). The MOCAGE horizontal resolution used for this study is 2° both in latitude and longitude and the model uses a semi-Lagrangian transport scheme. It includes 47 hybrid (σ, P) levels from the surface up to 5 hPa, where $\sigma = P/P_s$; P and P_s are the pressure and the surface pressure, respectively. MOCAGE has a vertical resolution of about 800 m in the vicinity of the tropopause and in the lower stratosphere, whereas in the boundary layer MOCAGE has 7 levels with a vertical resolution between 40 and 400 m. In the free troposphere, MOCAGE has a vertical resolution which varies from 400 to 800 m.

The assimilation module used in this study is PALM (Projet d'Assimilation par Logiciel Multi-méthode), a modular and flexible software, which consists of elementary components that exchange data (Lagarde et al., 2001). The technique implemented within PALM and used for the assimilation of MOPITT CO total columns, is the 3-D-FGAT

(First Guess at Appropriate Time) method. This method is a compromise between the 3-D-Var and 4-D-Var techniques (Fisher and Andersson, 2001). It compares the observation and background fields at the correct time and assumes that the increment to be added to the background state is constant over the entire assimilation window. The choice of this assimilation technique limits the size of the assimilation window, since it has to be short enough compared to chemistry and transport timescales. This technique has already produced good-quality results compared to independent data especially for O_3 and CO (e.g., Semane et al., 2007; El Amraoui et al., 2010; Claeyman et al., 2011b; Rabier et al., 2010; Bencherif et al., 2011).

The assimilation system MOCAGE-PALM has been used to assess the quality of satellite ozone measurements (Massart et al., 2007), and has been shown to overcome possible deficiencies in the model (e.g., Claeyman et al., 2010). Its assimilation product has been used in many atmospheric studies in relation to ozone loss in the Arctic vortex (El Amraoui et al., 2008a); tropics-midlatitudes exchange (Bencherif et al., 2007); exchange between the polar vortex and the midlatitudes (El Amraoui et al., 2008b); stratosphere-troposphere exchange (Semane et al., 2007; El Amraoui et al., 2010); and Observing Simulating System Experiment (OSSEs) studies (Claeyman et al., 2011a; Lahoz et al., 2012)

3 Assimilation of MOPITT CO total column: methodology and error specification

3.1 Assimilation methodology

For variational systems, the assimilation method is based on the minimization of the cost function, J:

$$J(x) = \frac{1}{2}\left[x(t_0) - x^{\mathrm{b}}(t_0)\right]^T \mathbf{B}^{-1}\left[x(t_0) - x^{\mathrm{b}}(t_0)\right] + \frac{1}{2}\sum_{i=1}^{p}[y_i - H_i(x)]^T \mathbf{R}_i^{-1}[y_i - H_i(x)] \quad (1)$$

AMTD
6, 6517–6566, 2013

CO total column assimilation

L. El Amraoui et al.

The first term on the right-hand side of Eq. (1) is the misfit to the background state and the second term represents the misfit to the observations. $x^b(t_0)$ and y_i are the background state at the initial time and the observation at time t_i, respectively. **B** and **R** are the background and the observation error covariance matrices, respectively. H is the observation operator, generally non-linear, which maps the model state x to the measurement space where y is located and p is the number of degrees of freedom.

For the incremental variational 3-D-FGAT method, the cost function, J in Eq. (1) can be expressed as:

$$J(\delta x) = \frac{1}{2}(\delta x)^T \mathbf{B}^{-1}(\delta x) + \frac{1}{2}\sum_{i=1}^{p}(d_i - \mathbf{H}_i(\delta x))^T \mathbf{R}_i^{-1}(d_i - \mathbf{H}_i(\delta x)) \tag{2}$$

δx is the increment vector which represents the difference between the model state x and the background state x^b ($\delta x = x - x^b$). The first term on the right-hand side is the background cost function, and the second term represents the observation cost function. $d = y - H(x^b)$ is the departure between the observation vector y and its model equivalent in observation space $H(x^b)$, and **H** represents the tangent-linear of the H operator.

For the assimilation of MOPITT data in this study, the observation vector y contains the CO total columns, while the model state x and, consequently, the background state x^b is the CO vertical profile updated by the model during the assimilation process. The observation operator H which maps the model state to the observation space is then a vertical integration over all model levels taking into account the vertical profile of both the pressure and the density of air. The minimization of the cost function J over each assimilation window is done in terms of total column between the observation vector (y) and the corresponding first guess (obtained by the integration of the vertical profile x^b in the model space). After each cycle over the assimilation window, the departure d, calculated in the observation space, is given as a total column. This increment in terms of total column is redistributed in the model space over the vertical profile of the model using $\mathbf{H}^T$, the transpose of the tangent-linear $\mathbf{H}$. Consequently, the assimilation of the CO total column impacts the whole vertical profile of the model, which will be updated to provide a new analysed state. The assimilation of MOPITT CO total column will then impact all of the vertical profile via the new analysed vertical profile. These vertical profiles calculated from CO TOTCOL_ANALYSES are validated by comparison to the vertical profiles of MOPITT V3 CO retrievals as well as to the vertical profiles deduced from the MOPITT CO PROFILE_ANALYSES taking into account their observation error covariance matrices and their averaging kernels.

3.2 Error specification

The first step of the proposed method consists in specifying the observation error covariance matrices. The assimilation process needs, at least, specification of the error covariance matrices ($\mathbf{R}$ and $\mathbf{B}$ matrices in Eqs. 1 and 2).

To validate the method, we assume in this study that the CO total column from MOPITT has no error covariance matrix or averaging kernel information. We specify the corresponding errors of the CO total columns based on the χ^2 test (e.g., El Amraoui et al., 2010): observation errors of the MOPITT CO total columns are estimated using this test. Different values of the observation error have been selected and several assimilation tests with these values have been conducted over a one-month study, August 2008. The appropriate value of the observation error is that for which the χ^2 test is the closest to 1. A value of χ^2 close to 1 indicates consistency between both error-covariance matrices ($\mathbf{R}$ and $\mathbf{B}$), whereas a value of χ^2 lower (greater) than 1 implies an overestimation (underestimation) of the observation and/or background errors.

Since the sensitivity of MOPITT measurements in the thermal infrared (TIR) wavelength depends, via the surface temperature and thermal contrast, on daytime and nighttime periods, specification of the measurement error is made by binning the observations according to day, night, land and sea. The specification of the errors will be done for three types of measurements: over land during daytime (LAND_DAY),

AMTD
6, 6517–6566, 2013

over land during nighttime (LAND_NIGHT) and over sea during daytime and nighttime (SEA). For each type of measurements we assume that all observations have the same percentage error and that errors are uncorrelated.

Figure 1 shows the time evolution of the χ^2 test over the period of study, August 2008 (left hand side) and the corresponding Gaussian fit of the normalized χ^2 test (right hand side) for different observation error values (diagonal of $\mathbf{R}$) corresponding to the measurement type LAND_DAY. We note that the χ^2 test is very sensitive to the observation error value. For low values of $\mathbf{R}$, the χ^2 test gives high values and vice-versa. The optimal observation error value (diagonal of $\mathbf{R}$) for which χ^2 is the closest to 1 for LAND_DAY measurements is $\sim 8\,\%$. Figure 2 is similar to Fig. 1 but for the LAND_NIGHT measurement type. The same conclusion about the behaviour of the χ^2 test as for LAND_DAY can be made, although the χ^2 test shows less variability. The optimal observation error value (diagonal of $\mathbf{R}$) for this type of measurement is about 11 %. For the SEA measurements, the corresponding χ^2 test is shown in Fig. 3, for which there is less temporal variability compared to the other two types of measurement. For this type of measurements (SEA), the χ^2 normalized distribution is more peaked compared to the other two types of measurement.

Table 1 summarizes the χ^2 results for all type of measurements. The optimal values of the observation error (diagonal of $\mathbf{R}$) are indicated in boldface. They are 8 %, 11 % and 7 % for LAND_DAY, LAND_NIGHT and SEA measurements, respectively. These values will be used as the observation error values for each corresponding type of measurements in the assimilation of MOPITT CO total column measurements.

3.3 A posteriori diagnostics

Each of the three types of MOPITT measurements (LAND_DAY, LAND_NIGHT and SEA) has been assimilated, in terms of total column, using the corresponding observation error selected according to the χ^2 test discussed in Sect. 3.2. Figure 4 shows the OMF and the OMA (observation minus analysis) diagnostics for MOPITT CO TOTCOL_ANALYSES for the whole assimilation period (August 2008). Figure 4-left shows the OMF distributions normalized by the observation errors for the three types of measurements. The OMF histograms are fitted by a Gaussian function. The comparison between the OMF histograms for all types of measurements and the corresponding fitted Gaussian function is very good. This good agreement supports the assumption that the specified observations and their corresponding forecasts have Gaussian errors. We note that the mean of all the normalized OMF values is positive but close to zero (lying between 0.4 and 0.7), which suggests that the bias between the model and the observations is very small for all the three types of measurements.

Figure 4-right shows the OMA and OMF histograms for all MOPITT CO total columns during the whole assimilation period. For the three types of measurements, the OMA histogram is narrower than that for OMF and the bias is reduced. Furthermore the standard deviation of OMA is smaller than that of OMF: σ_{OMA} = 4.9, 4.8 and 4.0 DU (Dobson Unit) for LAND_DAY, LAND_NIGHT and SEA measurements, respectively. The corresponding values for σ_{OMF} are: 14.1, 13.7 and 7.1 DU, respectively. This indicates that, as expected, the analyses for the different types of measurements are closer to the observations than the forecasts and the bias between the observations and the analyses is reduced.

4 Comparison of CO deduced from total column assimilation to MOPITT V3 observations

4.1 Validation in terms of horizontal maps at constant pressure levels

In this section we validate the vertical profiles calculated from MOPITT CO TOTCOL_ANALYSES in comparison to the MOPITT V3 CO observations in terms of vertical profiles at global and regional scales. Figure 5 presents a comparison in terms of longitude-latitude maps between MOPITT observations and those calculated from MOPITT CO TOTCOL_ANALYSES at the pressure levels of 700 and 250 hPa for LAND_DAY type of observations. Since the sensitivity of MOPITT measurements

AMTD
6, 6517–6566, 2013

through the averaging kernels is not vertically uniform, MOPITT TOTCOL_ANALYSES in terms of vertical profiles have been smoothed by the MOPITT V3 averaging kernels to take into account the vertical resolution as well as the a priori information used in the retrieval process of MOPITT vertical profiles. This is performed through the transformation of the vertical profile issued from MOPITT TOTCOL_ANALYSES (x_{assim}) using the averaging kernels of the MOPITT V3 vertical profiles (**A**) and the a priori CO profile (x_{apriori}) to create an analysed vertical profile (x_{comp}) appropriate for a quantitative comparison to the MOPITT V3 retrievals:

$$x_{\text{comp}} = \mathbf{A}x_{\text{assim}} + (\mathbf{I} - \mathbf{A})\,x_{\text{apriori}} \tag{3}$$

Note that both quantities: MOPITT observations and x_{comp} have been averaged in boxes of $2^\circ \times 2^\circ$ (corresponding to the grid mesh of the MOCAGE model) over the month of comparison, August 2008. Figure 5 shows that the general features of both datasets are consistent over the globe at 700 and 250 hPa and that the CO concentrations in the two fields have the same patterns particularly over the emission regions over central Africa, South-Eastern Asia and southern America. Generally, the fields of MOPITT TOTCOL_ANALYSES slightly overestimate CO concentrations, especially at 250 hPa. The maximum differences between both datasets for this type of measurements range from −12 % to 40 % for the 700 hPa pressure level with a mean bias of 15 %. Whereas, at the pressure level of 250 hPa, the differences range from −10 % to 25 % with a mean bias of 12 %. The mean differences between both datasets are higher at 700 hPa than at 250 hPa. This could be explained by the reduced sensitivity of MOPITT measurements at lower levels.

Figure 6 shows the same comparison as for Fig. 5 but for the LAND_NIGHT types (observations and analyses). The same conclusions as for Fig. 5 can be deduced concerning the general patterns, particularly over the CO emission regions. However, for this type of measurement, the MOPITT CO total column analyses in terms of longitude-latitude map are generally slightly overestimated at the two pressure levels. The mean differences are relatively small at 250 hPa compared to 700 hPa (between −25 % and

50 % for 700 hPa, and between −8 % and 12 % for 250 hPa). The mean bias between both datasets for this type of measurement is 18 % and 8 % for the pressure levels of 700 and 250 hPa, respectively. For this type of measurement, the mean difference at 700 hPa is higher than that of LAND_DAY measurements. This could be explained by the low sensitivity of MOPITT measurements in the lower troposphere in the TIR longwave radiation (Deeter et al., 2007). This sensitivity depends on the temperature differences between the ground and the troposphere (de Laat et al., 2010).

Figure 7 shows the same comparison as for Fig. 5 but for measurements performed over sea at the same pressure levels (700 and 250 hPa). At both levels, MOPITT total column analyses and MOPITT observations show the same patterns especially over the regions of CO outflow (e.g., equatorial Atlantic Ocean, northern Indian Ocean and northern Pacific Ocean) but with slightly different magnitudes. The mean difference at 700 hPa is larger than that at 250 hPa. At 250 hPa, the mean difference is relatively small (∼ 7 %) with a maximum value of about 14 %. At 700 hPa, the mean bias over all the globe is about 12 % with a maximum bias of about 33 % located near the regions of CO outflow. These results are consistent with the results found by Emmons et al. (2009) comparing MOPITT CO profiles with aircraft measurements at 700 and 250 hPa. They found that the bias is larger at lower levels, being on average 25 % and 9 % at 700 and 250 hPa, respectively.

4.2 Validation in terms of zonal means

In this section, we validate the CO vertical profiles calculated from MOPITT TOTCOL_ANALYSES in terms of zonal means by comparison to the MOPITT observations. Figure 8 shows, for the three types of measurements, CO monthly zonal means of MOPITT observations and their corresponding collocated MOPITT TOTCOL_ANALYSES in terms of vertical profiles for August 2008 at the pressure levels from the surface up to 150 hPa: the upper level of the MOPITT V3 observations. For the three types of measurements, the two zonal mean distributions (observation and TOTCOL_ANALYSES) show similar patterns. They both show the regions of CO emissions, particularly the

AMTD
6, 6517–6566, 2013

biomass burning region in the latitude range between 0° and 20° S as well as the CO emissions in the NH.

For LAND_DAY and LAND_NIGHT measurement types, the CO vertical extension is similar in both fields: over the emission regions, the maximum of CO extends up to 220 hPa over Africa and up to 150 hPa in the subtropical regions of the NH. These features of upper troposphere CO outflow reflect surface CO emissions lifted by convection. Nevertheless, MOPITT total column analyses slightly overestimate CO concentrations in the NH and in the tropical regions (up to: +30 % for LAND_NIGHT and +20 % for LAND_DAY). For the SEA measurement type, both zonal means have generally the same distributions. In the NH, both fields show high CO concentrations corresponding to the anthropogenic emissions over North America, Europe and Asia. However, in the SH the maximum difference between the two zonal means: MOPITT V3 observations and CO deduced from TOTCOL_ANALYSES for the SEA type of measurement ranges between −10 % and +20 %. Generally, in the SH both fields show very moderate CO concentrations reflecting very low CO emissions over this region.

4.3 Validation in terms of vertical profiles at regional scales

In this section, we validate the vertical profiles calculated from MOPITT CO TOTCOL_ANALYSES at different regional scales in comparison to MOPITT V3 observations. Figure 9 shows the main regional domains for which the evaluation of MOPITT total column analyses is done by comparison to MOPITT observations. These domains are considered as the regions having the bulk of the CO sources. The spatial extent of the regional areas in Fig. 9 for which the source emissions are significantly different is of the order of a few thousands of kilometres. This choice is consistent with the results of Liu et al. (2006) who state that the most important sources of CO variability in the troposphere are synoptic disturbances which have spatial scales of hundreds to thousands of kilometres. Consequently, it is important to have a statistical assessment of the variability of the two fields (MOPITT V3 observations and CO profiles deduced from TOTCOL_ANALYSES) over these regional areas. This will allow us to examine

AMTD
6, 6517–6566, 2013

their respective behaviour with respect to different types of emissions at the different regional scales.

Figure 10 presents a comparison in terms of vertical profiles between MOPITT V3 observations and their co-located profiles deduced from MOPITT CO TOTCOL_ANALYSES over the six domains of comparison. Both datasets are averaged over each domain for each of the 7 MOPITT levels (surface, 850, 700, 500, 350, 250 and 150 hPa). Over the six domains and for each type of observation, there is very good agreement between both datasets with corresponding standard deviations which are globally in agreement. Note also that, over the six domains, the CO concentrations over sea are generally lower than those over land, especially at lower levels. Over all the six domains of comparison, the two vertical profiles (MOPITT observations and those calculated from MOPITT CO TOTCOL_ANALYSES) are very similar and agree within the standard deviations of both datasets. Note also that the most significant variabilities of both datasets over all domains, especially domains 5, 6 and 3, are located at the lowermost levels (between the surface and 700 hPa). This reflects the variability of CO sources near the surface in Africa, South America and East Asia.

The mean bias as well as the mean RMS (Root Mean Square) between both datasets over the six domains of comparison for the three types of measurements are presented in Fig. 11 in percentage units. The absolute mean bias does not exceed 14 %, and is generally higher at lower levels (from the surface up to 700 hPa). For LAND_NIGHT and SEA types, the mean bias is generally positive for all domains at all pressure levels, reflecting an overestimation of the vertical profile deduced from MOPITT CO TOTCOL_ANALYSES in comparison with MOPITT V3 observations. The LAND_DAY type is generally characterized by a large positive bias with a corresponding RMS higher than that of other types particularly at the lowermost levels. This reflects a higher variability of MOPITT TOTCOL_ANALYSES for LAND_DAY compared to the other types of measurements.

For all types of measurements over all domains, both the bias and the RMS are large between the surface and 700 hPa. This is in agreement with the results of Fig. 10

AMTD
6, 6517–6566, 2013

showing high variability in this altitude range. From 500 hPa up to 150 hPa, both quantities have generally small values. The vertical profile of the correlation coefficient between both datasets over the six domains of comparison is presented in Fig. 12. The correlation coefficient ranges from ∼0.6 to 0.95. The correlation is generally good in the middle troposphere (at the pressure level of 500 hPa). This is in agreement with the fact that MOPITT measurements are very sensitive to this pressure level (Deeter et al., 2007). In the lowermost troposphere (between the surface and 700 hPa) the correlation coefficient is small ranging generally between 0.55 and 0.7, reflecting weaker agreement between the two datasets. This is in agreement with the fact that MOPITT observations are much more sensitive to the mid-troposphere than to the lower troposphere (Deeter et al., 2007). These results show that the vertical profiles calculated from MOPITT CO TOTCOL_ANALYSES and those of MOPITT V3 observations are generally in good agreement from the surface up to 150 hPa, particularly in the mid-troposphere.

5 Comparison of CO deduced from total column assimilation and CO deduced from vertical profile assimilation

In this section, we compare the vertical profiles calculated from MOPITT CO TOTCOL_ANALYSES for which the observation errors have been specified using the methodology based on the χ^2 test as presented in this paper (see: Sect. 3.2) and the vertical profiles issued from MOPITT V3 PROFILE_ANALYSES for which all the retrieval characteristics (averaging kernels and the observation error covariance matrices) are considered within the assimilation process. The objective is to quantify the differences between both analyses to further validate the method proposed in this paper concerning the assimilation of CO total column.

AMTD
6, 6517–6566, 2013

CO total column assimilation

L. El Amraoui et al.

5.1 Validation in terms of horizontal maps

In this section, we will validate the vertical profiles deduced from both analyses in terms of horizontal maps at constant pressure levels.

Figure 13 presents a comparison, at the pressure level of 700 hPa, between the vertical profiles calculated from MOPITT TOTCOL_ANALYSES with those obtained from MOPITT PROFILE_ANALYSES for which the averaging kernels and the observation error covariance matrices were taking into account. For this comparison, we consider the MOPITT PROFILE_ANALYSES as the reference because the vertical profiles are assimilated with all their retrieval characteristics. Consequently, they should present the most realistic state of the atmosphere. Thus, we evaluate the fields issued from TOTCOL_ANALYSES with respect to this reference field. Both fields are presented at global scale and averaged over the month of August 2008. The CO total column analyses and vertical profile analyses are very similar at the pressure level of comparison. The mean bias between both quantities over the globe is very low (~ 6 % in average). This mean bias is still in the range of the mean specified observation errors. Over some local areas, the maximum difference ranges between ~ -12 % and $\sim +14$ % which is lower compared to the results found by Emmons et al. (2009) where the bias between MOPITT retrievals and in-situ independent data can reach 35 %. Conversely, CO concentrations of these fields are different from that of the MOCAGE free run model highlighting the added value of the assimilation results (Fig. 13). For example, over the regions of South-America, central Africa and Asia, the free run results differ from both analyses at the specified pressure level (700 hPa). Figure 14 presents the same comparison as for Fig. 13 but at the pressure level of 200 hPa. The same conclusion as for the 700 hPa pressure level can be deduced: the profiles deduced from MOPITT TOTCOL_ANALYSES are very close to those issued from MOPITT PROFILE_ANALYSES with exactly the same patterns especially over the emission regions over Africa and south of Asia. The maximum mean bias between both fields is ranging between −3 and +10 %. However, the comparison between the model free run field and the vertical

AMTD
6, 6517–6566, 2013

profile analyses shows a bias which exceeds 60 % even if the general patterns between both fields are almost the same. These results confirm again that the CO fields deduced, in one hand from MOPITT PROFILE_ANALYSES taking into account both the corresponding error covariance matrices and their averaging kernels and, in the other hand those deduced from CO TOTCOL_ANALYSES with the error covariance matrices specified using the simplified method described in this paper are almost the same with very small differences. The relative mean bias between both datasets is very small and is generally within the specified errors.

5.2 Validation in terms of zonal means

In this section, we evaluate the differences between the two analyses in terms of zonal means. In this way, we present in Fig. 15 a comparison of CO zonal mean fields between the PROFILE_ANALYSES, TOTCOL_ANALYSES and the MOCAGE free run model. The CO distribution is similar for both analyses (total column and vertical profiles). Over the SH in the extratropics both fields show moderate values of CO from the surface up to the mid-troposphere (∼ 400 hPa). CO concentrations calculated from MOPITT TOTCOL_ANALYSES are slightly overestimated compared to those calculated from MOPITT PROFILE_ANALYSES. The mean bias between both analyses (Fig. 15-Middle-right) is positive and does not exceed 15% over the vertical. In the tropics, both fields show strong CO emissions over Africa that can reach the pressure level of ∼ 200 hPa. Over this region, the differences between the two fields are very small ranging from −5 % to +9 %. In the NH, the two fields show very high CO concentrations in the mid-troposphere. These high CO concentrations correspond to anthropogenic emissions from North America, Europe and East Asia. The mean bias between both analyses ranges between −12 and +12 % which shows that both fields are very similar over the altitude range from the surface up to 150 hPa. However, the comparison between the zonal means deduced from MOPITT PROFILE_ANALYSES against those of the MOCAGE model free run (Fig. 15-Bottom) shows a bias ranging between −35 % and 45 %, particularly in the mid-troposphere of the tropical regions and the lower troposphere of the extra-tropics (< 40 %). These results show that the information derived from the total columns using data assimilation is capable of modifying the vertical structure of the CO distribution over the whole troposphere, showing features very similar to those obtained from the assimilation of MOPITT V3 CO vertical profiles.

5.3 Evaluation in terms of vertical profiles at regional scales

In this section, we evaluate the differences between the two analyses in terms of vertical profiles at regional scales. We compare, at the same regional scales shown in Fig. 9, the vertical profiles obtained from MOPITT CO TOTCOL_ANALYSES, and those obtained from MOPITT CO PROFILE_ANALYSES taking into account their corresponding characteristics (error covariance matrices and averaging kernels). The vertical profiles calculated from both analyses are averaged over different domains for August 2008. Figure 16 presents the results of CO vertical profiles with their associated standard deviations. The standard deviation represents the variability of the CO concentration over each domain for the month of August 2008. The profiles calculated from both analyses as well as their associated standard deviations are similar for all domains.

Both analyses show the same behaviour for the CO fields in terms of vertical structure at the regional scales, and have similar variability. The maximum standard deviation is generally found at pressure levels between the surface and 700 hPa for both analyses, especially for domains 5 (Africa), 6 (South America), and 3 (East Asia). This is in good agreement with the results of Fig. 11 which illustrates again the variability of CO sources over Africa, South America and East Asia. Figure 16 confirms that the analyses obtained from TOTCOL_ANALYSES and those obtained from PROFILE_ANALYSES give almost the same vertical structure over regional scales. This shows that the assimilation of total column impacts all the vertical levels of the profile in the same way as the assimilation of the vertical profiles.

AMTD

6, 6517–6566, 2013

CO total column assimilation

L. El Amraoui et al.

Figure 17 presents the vertical profiles of the mean bias and the mean RMS both in percent between the two assimilation set-ups (TOTCOL_ANALYSES and PROFILE_ANALYSES) averaged over each domain for the month of August 2008. For all regional domains, the mean bias has low values at all pressure levels and is generally less than 10% except for domains 2 (Europe) and 3 (East Asia) at 150 hPa, where it reaches ~ 13 %. The values of the RMS range between +10 % and +15 % for most domains. All these values are smaller or in the range of the expected errors of the assimilation results, and are generally smaller than the observation error values used in the assimilation process. The only exception concerns domain 6 (South America), for which the mean RMS is about 20 % in the altitude range between the surface and 400 hPa. This could be attributed to the large variability of the CO field in this domain (see Fig. 15). The vertical profiles of the correlation coefficient between the two analyses over the six domains of comparison are presented in Fig. 18. For the different domains, the correlation coefficients range between 0.75 and 0.99, with most of the values close to 0.9. This shows a very good agreement between the two assimilation results.

The results shown in this section concern the following statistics calculated between both datasets: bias, RMS and correlation coefficient. They show that the comparison between the vertical profiles obtained from MOPITT CO TOTCOL_ANALYSES and those obtained from MOPITT CO PROFILE_ANALYSES taking into account the corresponding averaging kernels and the error covariance matrices are consistent. Both analyses are in very good agreement at the global and regional scales.

6 Conclusions

The aim of this paper is to show the benefit of using satellite CO total column data with no associated error covariance matrices and averaging kernels within an assimilation system. The total column analyses permit us to give relevant information on the vertical structure of the CO field at global and regional scales.

AMTD
6, 6517–6566, 2013
CO total column assimilation
L. El Amraoui et al.

The method described in this paper consists in estimating the observation error covariance matrices (diagonal of the **R** matrix) and obtaining realistic CO analyses. The method for estimating the error covariance matrices is based on the use of the χ^2 test to obtain consistency between model and observation errors. The method has been applied to the MOPITT version 3 (V3) CO total column for which the vertical profiles obtained by data assimilation using the MOCAGE-PALM assimilation system have been compared to the MOPITT CO vertical profiles taking into account the averaging kernels as well as the a priori profile of MOPITT retrievals.

The specification of the errors for the CO total column before assimilation has been done by discriminating the observations according to day, night, land and sea. This discrimination is motivated by the fact that the sensitivity of MOPITT measurements in the thermal infrared wavelength depends, via surface temperature and thermal contrast, on daytime and nighttime periods. The appropriate values of the observation errors for which the χ^2 is the closest to 1 are 8% and 11 % for measurements performed over land during daytime (LAND_DAY) and over land during night (LAND_NIGHT), respectively. For measurements performed over sea during daytime and nighttime (SEA), the nominal observation error is estimated to be 7 %. The a posteriori diagnostics concerning the analysed fields for all specified total column observations allow us to deduce that the specified observations errors using the proposed method as well as the corresponding forecasts error, have a Gaussian structure.

To validate the method described in this paper, the analyses derived from CO total columns were compared initially with MOPITT V3 observations. The objective of this first comparison is to assess the capacity of the method to derive the same vertical profiles. In a second step, the same CO total column analyses were compared with the analyses obtained from the assimilation of vertical profiles with their characteristic parameters: error covariance matrices and averaging kernels. The objective of this second comparison is to evaluate the differences between the two analyses and, therefore, measure the usefulness of the method to readily produce good quality CO analyses.

AMTD
6, 6517–6566, 2013

In the first comparison, both CO total column analyses and MOPITT observations show similar patterns concerning the CO concentrations for the three types of measurements in terms of longitude–latitude maps. The mean bias at 700 hPa between both datasets is 15 %, 18 % and 12 % for LAND_DAY, LAND_NIGHT and SEA types, respectively. At 250 hPa, the patterns between both fields are also consistent. The respective mean biases are positive and they are +12 %, +8 % and +7 % for LAND_DAY, LAND_NIGHT and SEA types, respectively. The comparison of the zonal means shows that the vertical extension is homogeneous in both fields from the surface up to 150 hPa for the three types of measurements. At regional scales, the comparison of the two datasets in terms of vertical profiles shows very good agreement. The mean bias does not exceed +10 % and is generally large at low levels which could be attributed to the variability of CO sources near the surface. The vertical profile of the correlation coefficient between both fields ranges from 0.6 to 0.95 over all pressure levels of the MOPITT retrievals.

In the second comparison, the analyses deduced from the MOPITT vertical profiles considering their averaging kernels and error covariance matrices and the CO total column analyses show very good agreement over the globe. The general aspect of both datasets is consistent at global scale and presents the same features in the CO concentrations particularly over the emission regions in central Africa, South-Eastern Asia and Southern America. The absolute differences between both datasets are higher at 700 hPa than at 200 hPa. The mean bias between both datasets is 6 % and 8 % at the pressure levels of 700 and 200 hPa, respectively. In terms of zonal means, the CO distribution is similar for both analyses with very low differences. The total column analyses tend to slightly overestimate the CO concentrations. The maximum mean bias does not exceed 15 % over all pressure levels. Over regional scales, the comparison in terms of vertical profiles calculated from both analyses as well as their standard deviations are in very good agreement. The mean bias is very small and generally does not exceed +10 %, whereas the vertical profile of the correlation coefficient ranges from 0.75 to 0.99 over all pressure levels. These results concerning the CO distributions,

AMTD
6, 6517–6566, 2013
CO total column assimilation
L. El Amraoui et al.

vertical profiles, mean bias, RMS and correlation coefficient, confirm that the analyses deduced from the assimilation of CO total columns are in very good agreement with the analyses calculated from the assimilation of the MOPITT CO vertical profiles taking into account all the retrieval characteristic parameters. This agreement is confirmed both at global and regional scales.

The method developed in this paper deals only with the assimilation of CO total columns. The validation of the method was carried out over one month period with a characterization of the error based on the discrimination of the measurements with respect to those carried out during daytime and nighttime over land and sea. This method will be generalized to other periods with further work on the characterization of the error. Besides for chemical species that can be measured only as total column, this method is a good alternative to assess their vertical profile in the troposphere.

The proposed method will be applied to the operational CO total column from IASI as provided by EUMETSAT. Note that, as part of future satellite missions with large volumes of data that would require quasi-operational treatment, the results of this study could be used for the ready calculation of the three-dimensional distribution of CO as well as other tropospheric species, with relatively very low cost.

Acknowledgements. This work is funded in France by the Centre National de Recherches Météorologiques (CNRM) of Météo-France and the Centre National de Recherches Scientifiques (CNRS). W. Lahoz is supported by the RTRA/STAE fondation under the POGEQA project. The authors acknowledge ETHER, the French atmospheric composition database (CNES and CNRS-INSU) and the Région Midi-Pyrénées (INFOAIR project).

The publication of this article is financed by CNRS-INSU.

AMTD
6, 6517–6566, 2013

References

Beer, R., Glavich, T. A., and Rider, D. M.: Tropospheric emission spectrometer for the Earth Observing System's Aura Satellite, Appl. Optics, 40, 2356–2367, 2001. 6520

Bencherif, H., El Amraoui, L., Semane, N., Massart, S., Charyulu, D. V., Hauchecorne, A., and Peuch, V. H.: Examination of the 2002 major warming in the southern hemisphere using ground-based and Odin/SMR assimilated data: stratospheric ozone distributions and tropic/mid-latitude exchange, Can. J. Phys., 85, 1287–1300, doi:10.1139/P07-143, 2007. 6525

Bencherif, H., El Amraoui, L., Kirgis, G., Leclair De Bellevue, J., Hauchecorne, A., Mzé, N., Portafaix, T., Pazmino, A., and Goutail, F.: Analysis of a rapid increase of stratospheric ozone during late austral summer 2008 over Kerguelen (49.4° S, 70.3° E), Atmos. Chem. Phys., 11, 363–373, doi:10.5194/acp-11-363-2011, 2011. 6525

Bian, H., Chin, M., Kawa, S. R., Duncan, B., Arellano, A., and Kasibhatla, P.: Sensitivity of global CO simulations to uncertainties in biomass burning sources, J. Geophys. Res., 112, D23308, doi:10.1029/2006JD008376, 2007. 6520

Bovensmann, H., Burrows, J.-P., Buchwitz, M., Frerick, J., Noel, S., Rozanov, V. V., Chance, K. V., and Goede, A. P. H.: SCIAMACHY: Mission objectives and measurement modes, J. Atmos. Sci., 56, 127–150, 1999. 6520

Bremer, H., Kar, J., Drummond, J. R., Nichitu, F., Zou, J., Liu, J., Gille, J. C., Deeter, M. N., Francis, G., Ziskin, D., and Warner, J.: Spatial and temporal variation of MOPITT CO in Africa and South America: A comparison with SHADOZ ozone and MODIS aerosol, J. Geophys. Res.-Atmos., 109, D12304, doi:10.1029/2003JD004234, 2004. 6523

Claeyman, M., Attié, J.-L., El Amraoui, L., Cariolle, D., Peuch, V.-H., Teyssèdre, H., Josse, B., Ricaud, P., Massart, S., Piacentini, A., Cammas, J.-P., Livesey, N. J., Pumphrey, H. C., and Edwards, D. P.: A linear CO chemistry parameterization in a chemistry-transport model: evaluation and application to data assimilation, Atmos. Chem. Phys., 10, 6097–6115, doi:10.5194/acp-10-6097-2010, 2010. 6521, 6524, 6525

Claeyman, M., Attié, J.-L., Peuch, V.-H., El Amraoui, L., Lahoz, W. A., Josse, B., Joly, M., Barré, J., Ricaud, P., Massart, S., Piacentini, A., von Clarmann, T., Höpfner, M., Orphal, J., Flaud, J.-M., and Edwards, D. P.: A thermal infrared instrument onboard a geostationary platform for CO and O_3 measurements in the lowermost troposphere: Observing System

Simulation Experiments (OSSE), Atmos. Meas. Tech., 4, 1637–1661, doi:10.5194/amt-4-1637-2011, 2011a. 6525

Claeyman, M., Attié, J.-L., Peuch, V.-H., El Amraoui, L., Lahoz, W. A., Josse, B., Ricaud, P., von Clarmann, T., Höpfner, M., Orphal, J., Flaud, J.-M., Edwards, D. P., Chance, K., Liu, X., Pasternak, F., and Cantié, R.: A geostationary thermal infrared sensor to monitor the lowermost troposphere: O_3 and CO retrieval studies, Atmos. Meas. Tech., 4, 297-317, doi:10.5194/amt-4-297-2011, 2011b. 6524, 6525

Clerbaux, C., Hadji-Lazaro, J., Hauglustaine, D., Megie, G., Khattatov, B., and Lamarque, J.-F.: Assimilation of carbon monoxide measured from satellite in a three-dimensional chemistry-transport model, J. Geophys. Res., 106, 15385–15394, 2001. 6519, 6521

Courtier, P., Freydier, C., Geleyn, J., Rabier, F., and Rochas, M.: The ARPEGE project at Météo France, in: Atmospheric Models, Vol. 2, 193–231, Workshop on Numerical Methods, Reading, UK, 1991. 6524

Crutzen, P. J. and Andreae, M. O.: Biomass Burning in the Tropics: Impact on Atmospheric Chemistry and Biogeochemical Cycles, Science, 250, 1669–1678, doi:10.1126/science.250.4988.1669, 1990. 6519

Deeter, M. N., Edwards, D. P., Gille, J. C., and Drummond, J. R.: Sensitivity of MOPITT observations to carbon monoxide in the lower troposphere, J. Geophys. Res.-Atmos., 112, D24306, doi:10.1029/2007JD008929, 2007. 6523, 6531, 6534

de Laat, A. T. J., Gloudemans, A. M. S., Aben, I., and Schrijver, H.: Global evaluation of SCIAMACHY and MOPITT carbon monoxide column differences for 2004–2005, J. Geophys. Res., 115, D06307, doi:10.1029/2009JD012698, 2010. 6531

Drummond, J. and Mand, G.: The measurements of pollution in the troposphere (MOPITT) instrument: Overall performance and calibration requirements, J. Atmos. Ocean. Tech., 13, 314–320, 1996. 6519, 6522

Dufour, A., Amodei, M., Ancellet, G., and Peuch, V.-H.: Observed and modelled “chemical weather” during ESCOMPTE, Atmos. Res., 74, 161–189, 2004. 6524

Edwards, D. P., Emmons, L. K., Hauglustaine, D. A., Chu, D. A., Gille, J. C., Kaufman, Y. J., Pétron, G., Yurganov, L. N., Giglio, L., Deeter, M. N., Yudin, V., Ziskin, D. C., Warner, J., Lamarque, J.-F., Francis, G. L., Ho, S. P., Mao, D., Chen, J., Grechko, E. I., and Drummond, J. R.: Observations of carbon monoxide and aerosols from the Terra satellite: Northern Hemisphere variability, J. Geophys. Res.-Atmos., 109, D24202, doi:10.1029/2004JD004727, 2004. 6523

El Amraoui, L., Peuch, V.-H., Ricaud, P., Massart, S., Semane, N., Teyssèdre, H., Cariolle, D., and Karcher, F.: Ozone loss in the 2002–2003 Arctic vortex deduced from the assimilation of Odin/SMR O_3 and N_2O measurements: N_2O as a dynamical tracer, Q. J. Roy. Meteorol. Soc., 134, 217–228, 2008a. 6524, 6525

El Amraoui, L., Semane, N., Peuch, V.-H., and Santee, M. L.: Investigation of dynamical processes in the polar stratospheric vortex during the unusually cold winter 2004/2005, Geophys. Res. Lett., 35, L03803, doi:10.1029/2007GL031251, 2008b. 6524, 6525

El Amraoui, L., Attié, J.-L., Semane, N., Claeyman, M., Peuch, V.-H., Warner, J., Ricaud, P., Cammas, J.-P., Piacentini, A., Josse, B., Cariolle, D., Massart, S., and Bencherif, H.: Midlatitude stratosphere – troposphere exchange as diagnosed by MLS O_3 and MOPITT CO assimilated fields, Atmos. Chem. Phys., 10, 2175–2194, doi:10.5194/acp-10-2175-2010, 2010. 6521, 6524, 6525, 6527

Emmons, L., Deeter, M., Gille, J., Edwards, D., Attié, J.-L., Warner, J., Ziskin, D., Francis, G., Khattatov, B., Lamarque, V. Y. J.-F., Ho, S., Mao, D., Chen, J., Drummond, J., Novelli, P., Sachse, G., Coffey, M., Hannigan, J., Gerbig, C., Kawakami, S., Kondo, Y., Takegawa, N., Schlager, H., Baehr, J., and Ziereis, H.: Validation of Measurements of Pollution in the Troposphere (MOPITT) CO retrievals with aircraft in situ profiles, J. Geophys. Res., 109, D03309, doi:10.1029/2003JD004101, 2004. 6523

Emmons, L. K., Pfister, G. G., Edwards, D. P., Gille, J. C., Sachse, G., Blake, D., Wofsy, S., Gerbig, C., Matross, D., and Nédélec, P.: Measurements of Pollution in the Troposphere (MOPITT) validation exercises during summer 2004 field campaigns over North America, J. Geophys. Res.-Atmos., 112, D12S02, doi:10.1029/2006JD007833, 2007. 6523

Emmons, L. K., Edwards, D. P., Deeter, M. N., Gille, J. C., Campos, T., Nédélec, P., Novelli, P., and Sachse, G.: Measurements of Pollution In The Troposphere (MOPITT) validation through 2006, Atmos. Chem. Phys., 9, 1795–1803, doi:10.5194/acp-9-1795-2009, 2009. 6523, 6531, 6535

Fisher, M. and Andersson, E.: Developments in 4D-Var and Kalman filtering, in: Technical Memorandum No. 347, p. 36, Research Department, ECMWF, Reading, UK, 2001. 6525

Granier, C., Petron, G., Muller, J. F., and Brasseur, G.: The impact of natural and anthropogenic hydrocarbons on the tropospheric budget of carbon monoxide, Atmos. Environ., 34, 5255–5270, 2000. 6519

Heald, C. L., Jacob, D. J., Jones, D. B. A., Palmer, P. I., Logan, J. A., Streets, D. G., Sachse, G. W., Gille, J. C., Hoffman, R. N., and Nehrkorn, T.: Comparative inverse analysis of satellite

(MOPITT) and aircraft (TRACE-P) observations to estimate Asian sources of carbon monoxide, J. Geophys. Res.-Atmos., 109, D23306, doi:10.1029/2004JD005185, 2004. 6523

Jones, D., Bowman, K. W., Palmer, P., Worden, J., Jacob, D., Hoffman, R., Bey, I., and Yantosca, R.: Potential of observations from the Troposphere Emission Spectrometer to constrain continental sources of carbon monoxide, J. Geophys. Res., 108, 4789, doi:10.1029/2003JD003702, 2003. 6520

Lagarde, T., Piacentini, A., and Thual, O.: A new representation of data-assimilation methods: The PALM flow-charting approach, Q. J. Roy. Meteorol. Soc., 127, 189–207, 2001. 6524

Lahoz, W. A., Geer, A. J., Bekki, S., Bormann, N., Ceccherini, S., Elbern, H., Errera, Q., Eskes, H. J., Fonteyn, D., Jackson, D. R., Khattatov, B., Marchand, M., Massart, S., Peuch, V.-H., Rharmili, S., Ridolfi, M., Segers, A., Talagrand, O., Thornton, H. E., Vik, A. F., and von Clarmann, T.: The Assimilation of Envisat data (ASSET) project, Atmos. Chem. Phys., 7, 1773–1796, doi:10.5194/acp-7-1773-2007, 2007. 6524

Lahoz, W. A., Peuch, V.-H., Orphal, J., Attie, J.-L., Chance, K., Liu, X., Edwards, D., Elbern, H., Flaud, J.-M., Claeyman, M., and El Amraoui, L.: Monitoring Air Quality from space: The case for the geostationary platform, B. Am. Meteorol. Soc., 93, 221–233, doi:10.1175/BAMS-D-11-00045.1, 2012. 6525

Lamarque, J.-F., Khattatov, B., Gille, J., and Brasseur, G.: Assimilation of MAPS CO in a global three-dimensional model, J. Geophys. Res., 104, 26209–26218, doi:10.1029/1999JD900807, 1999. 6521

Li, Q., Jiang, J., Wu, D., Read, W., Livesey, N., Waters, J., Zhang, Y., Wang, B., Filipiak, M., Davis, C., Turquety, S., Wu, S., Park, R., Yantosca, R. M., and Jacob, D.: Convective outflow of South Asian pollution: A global CTM simulation compared with EOS MLS observations, Geophys. Res. Lett., 32, L14826, doi:10.1029/2005GL022762, 2005. 6523

Liu, J., Drummond, J. R., Jones, D. B. A., Cao, Z., Bremer, H., Kar, J., Zou, J., Nichitiu, F., and Gille, J. C.: Large horizontal gradients in atmospheric CO at the synoptic scale as seen by spaceborne Measurements of Pollution in the Troposphere, J. Geophys. Res., 111, D02306, doi:10.1029/2005JD006076, 2006. 6532

Mahieu, E., Zander, R., Delbouille, L., Demoulin, P., Roland, G., and Servais, C.: Observed trends in total vertical column abundances of atmospheric gases from IR solar spectra recorded at the Jungfraujoch, J. Atmos. Chem., 28, 227–243, doi:10.1023/A:1005854926740, 1997. 6519

Massart, S., Piacentini, A., Cariolle, D., El Amraoui, L., and Semane, N.: Assessment of the quality of the ozone measurements from the Odin/SMR instrument using data assimilation, Can. J. Phys., 85, 1209–1223, 2007. 6525

McMillan, W., Barnet, C., Strow, L., Chahine, M., McCourt, M., Warner, J., Novelli, P., Korontzi, S., Maddy, E., and Datta, S.: Daily global maps of carbon monoxide from NASA's Atmospheric Infrared Sounder, Geophys. Res. Lett., 32, L11801, doi:10.1029/2004GL021821, 2005. 6520

Pétron, G., Granier, C., Khattatov, B., Yudin, V., Lamarque, J.-F., Emmons, L., Gille, J., and Edwards, D. P.: Monthly CO surface sources inventory based on the 2000–2001 MOPITT satellite data, Geophys. Res. Lett., 31, L21107, doi:10.1029/2004GL020560, 2004. 6523

Peuch, V.-H., Amodei, M., Barthet, T., Cathala, M. L., Michou, M., and Simon, P.: MOCAGE, MOdéle de Chimie Atmosphérique à Grande Echelle, in: Proceedings of Météo France: Workshop on atmospheric modelling, 33–36, Toulouse, France, December 1999. 6524

Pradier, S., Attié, J.-L., Chong, M., Escobar, J., Peuch, V.-H., Lamarque, J.-F., Khattatov, B., and Edwards, D.: Evaluation of 2001 springtime CO transport over West Africa using MOPITT CO measurements assimilated in a global chemistry transport model, Tellus B, 58, 163–176, 2006. 6521

Rabier, F., Bouchard, A., Brun, E., Doerenbecher, A., Guedj, S., Guidard, V., Karbou, F., Peuch, V., El Amraoui, L., Puech, D., Genthon, C., Picard, G., Town, M., Hertzog, A., Vial, F., Cocquerez, P., Cohn, S., Hock, T., Fox, J., Cole, H., Parsons, D., Powers, J., Romberg, K., VanAndel, J., Deshler, T., Mercer, J., Haase, J., Avallone, L., Kalnajs, L., Mechoso, C., Tangborn, A., Pellegrini, A., Frenot, Y., Thépaut, J.-N., McNally, A., Balsamo, G., and Steinle, P.: The Concordiasi Project in Antarctica, B. Am. Meteorol. Soc., 91, 69–86, doi:10.1175/2009BAMS2764.1, 2010. 6525

Reichle, H. G., Anderson, B. E., Connors, V. S., Denkins, T. C., Forbes, D. A., Gormsen, B. B., Langenfelds, R. L., Neil, D. O., Nolf, S. R., Novelli, P. C., Pougatchev, N. S., Roell, M. M., and Steele, L. P.: Space shuttle based global CO measurements during April and October 1994, MAPS instrument, data reduction, and data validation, J. Geophys. Res., 104, 21443–21454, 1999. 6519

Ricaud, P., Attié, J.-L., Teyssèdre, H., El Amraoui, L., Peuch, V.-H., Matricardi, M., and Schluessel, P.: Equatorial total column of nitrous oxide as measured by IASI on MetOp-A: implications for transport processes, Atmos. Chem. Phys., 9, 3947–3956, doi:10.5194/acp-9-3947-2009, 2009a. 6524

Ricaud, P., Pommereau, J.-P., Attié, J.-L., Le Flochmoën, E., El Amraoui, L., Teyssèdre, H., Peuch, V.-H., Feng, W., and Chipperfield, M. P.: Equatorial transport as diagnosed from nitrous oxide variability, Atmos. Chem. Phys., 9, 8173–8188, doi:10.5194/acp-9-8173-2009, 2009b. 6524

Rodgers, C.: Inverse Methods for Atmospheric Sounding: Theory and Practice, Series on Atmospheric, Oceanic and Planetary Physics, Vol. 2, 238 pp., World Scientific, Hackensack, New Jersey, 2000. 6522

Semane, N., Peuch, V.-H., El Amraoui, L., Bencherif, H., Massart, S., Cariolle, D., Attié, J.-L., and Abida, R.: An observed and analysed stratospheric ozone intrusion over the high Canadian Arctic UTLS region during the summer of 2003, Q. J. Roy. Meteorol. Soc., 133, 171–178, 2007. 6524, 6525

Semane, N., Peuch, V.-H., Pradier, S., Desroziers, G., El Amraoui, L., Brousseau, P., Massart, S., Chapnik, B., and Peuch, A.: On the extraction of wind information from the assimilation of ozone profiles in Météo-France 4-D-Var operational NWP suite, Atmos. Chem. Phys., 9, 4855–4867, doi:10.5194/acp-9-4855-2009, 2009. 6524

Tangborn, A., Stajner, I., Buchwitz, M., Khlystova, I., Pawson, S., Burrows, J., Hudman, R., and Nedelec, P.: Assimilation of SCIAMACHY total column CO observations: Global and regional analysis of data impact, J. Geophys. Res., 114, D07307, doi:10.1029/2008JD010781, 2009. 6521

Yurganov, L. N., McMillan, W. W., Dzhola, A. V., Grechko, E. I., Jones, N. B., and van der Werf, G. R.: Global AIRS and MOPITT CO measurements: Validation, comparison, and links to biomass burning variations and carbon cycle, J. Geophys. Res.-Atmos., 113, D09301, doi:10.1029/2007JD009229, 2008. 6523

Zheng, Y. G., Zhu, P. J., Chan, C. Y., Chan, L. Y., Cui, H., Zheng, X. D., Zhao, Q., and Qin, Y.: Influence of biomass burning in Southeast Asia on the lower tropospheric ozone distribution over South China, Chinese J. Geophys.-Ch., 47, 767–775, 2004. 6523

Table 1. Mean and median values of χ^2 test for different error values of MOPITT V3 total column observations. The error values of the observations for which the χ^2 test is the closest to 1 are indicated in boldface. They are 8 % for LAND_DAY; 11 % for LAND_NIGHT and 7 % for SEA. These error values are fixed within the assimilation system for all experiments concerning MOPITT V3 total columns.

				χ^2				
	LAND_DAY			LAND_NIGHT			SEA	
R (%)	Mean value	Median value	R (%)	Mean value	Median value	R (%)	Mean value	Median value
4	4.37	3.98	8	2.15	2.04	4	2.59	2.54
5	2.66	2.36	9	1.60	1.51	5	1.70	1.67
6	1.78	1.59	10	1.15	1.16	6	1.26	1.24
7	1.27	1.18	**11**	**1.05**	**1.01**	**7**	**0.96**	**0.94**
8	**0.97**	**0.92**	12	0.85	0.79	8	0.75	0.74
9	0.78	0.72	13	0.72	0.68	9	0.51	0.50

AMTD
6, 6517–6566, 2013

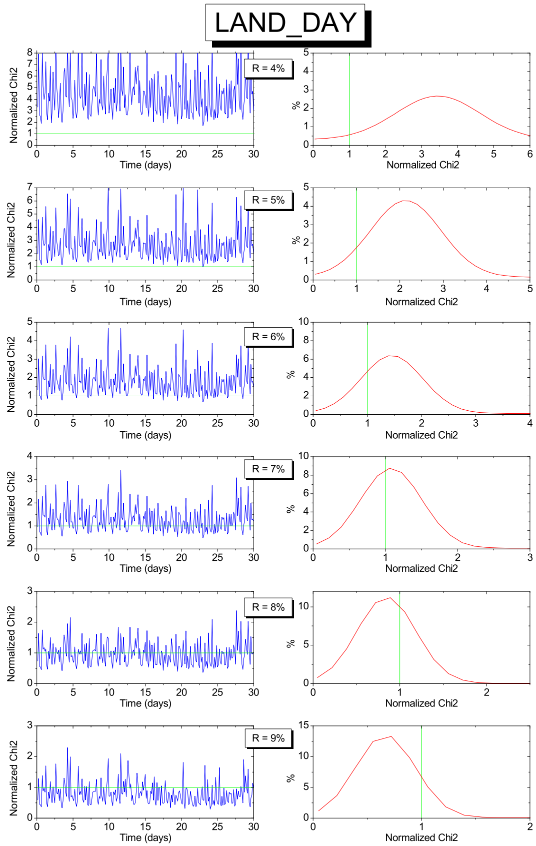

Fig. 1. (Left): time evolution of the normalized χ^2 value over the month of August 2008 for different values of observation error concerning MOPITT V3 total column made over land during daytime (LAND_DAY). (Right): the Gaussian fit of the corresponding normalized histogram. The mean as well as the median values of χ^2 for each observation error value are reported in Table 1.

AMTD
6, 6517–6566, 2013

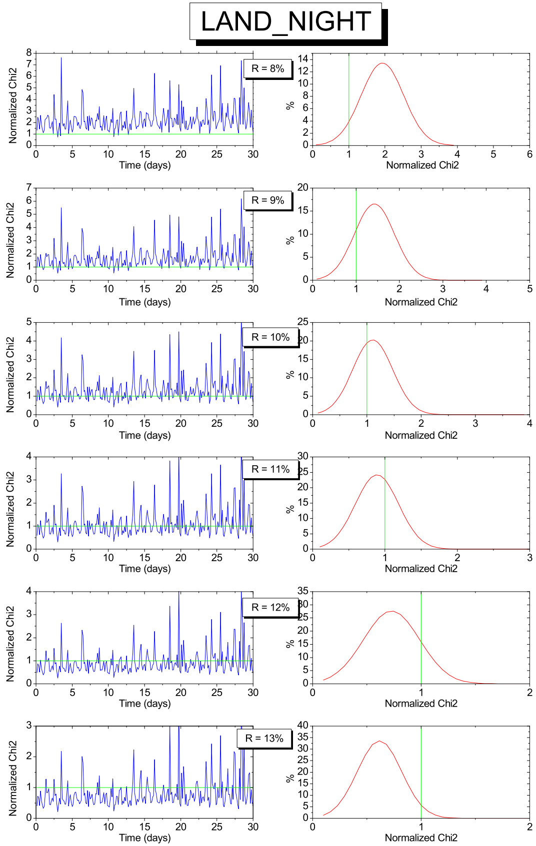

Fig. 2. Same as Fig. 1 but for MOPITT CO total column observations carried out over land during nighttime (LAND_NIGHT).

AMTD
6, 6517–6566, 2013

CO total column assimilation

L. El Amraoui et al.

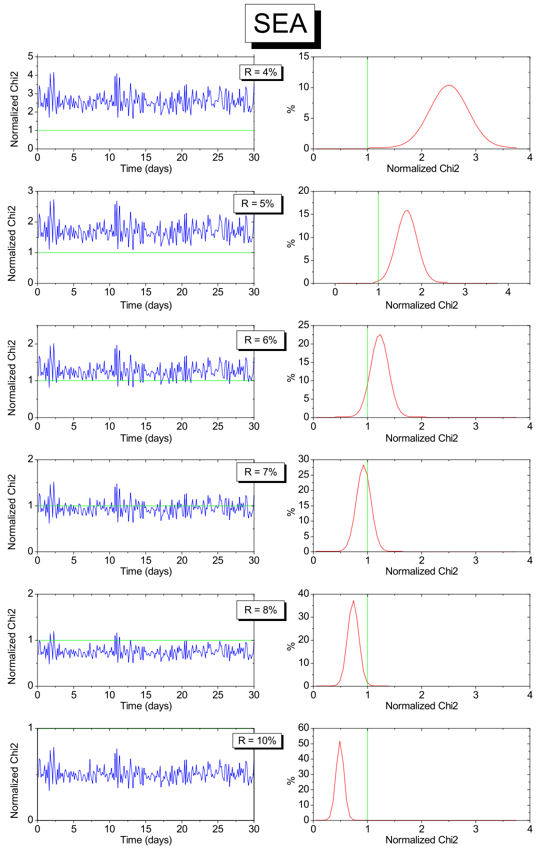

Fig. 3. Same as Fig. 2 but for MOPITT CO total column observations carried out over sea during daytime and nighttime (SEA).

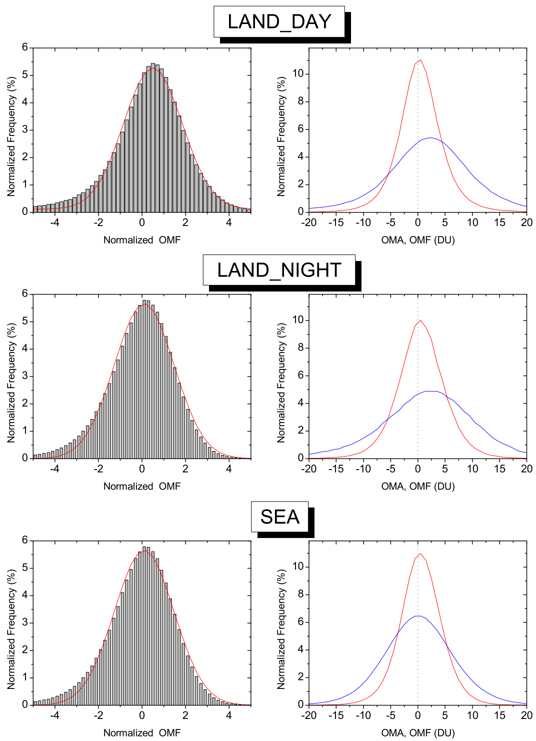

Fig. 4. A posteriori verification of the observation error specification for the analyses issued from the MOPITT CO total column for which the observation errors are estimated using the proposed method. (Left): histograms of OMF (Observations Minus Forecast) differences normalized by the specified observation errors. The red line is a Gaussian fit to the histogram. The good agreement between the histogram and the fit function supports the assumption of Gaussian errors in the observations and the forecast. (Right): histograms of Observations Minus Analysis (OMA: red lines) and OMF (blue lines).

AMTD
6, 6517–6566, 2013

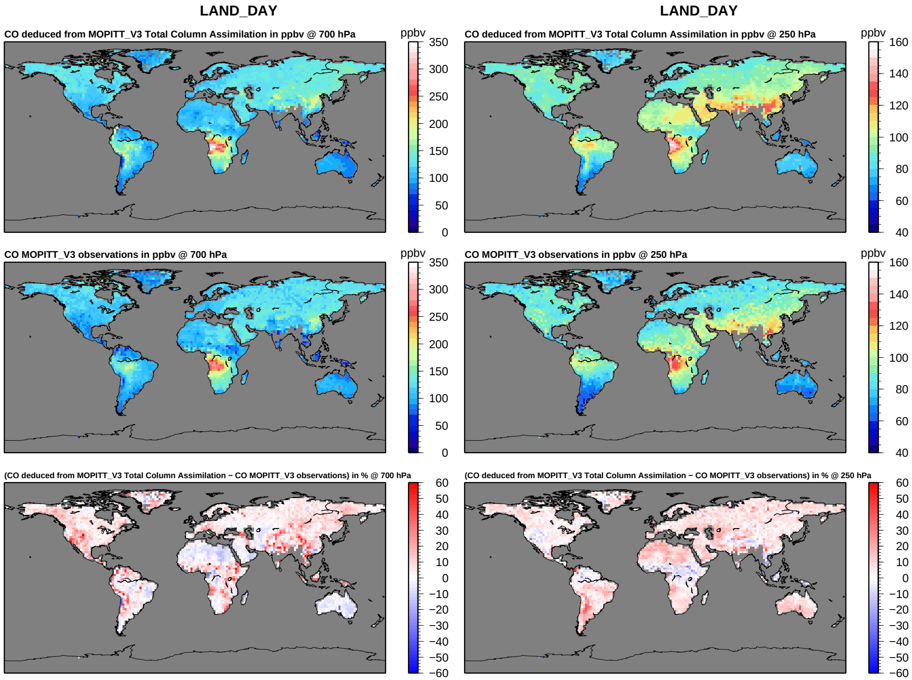

Fig. 5. Comparison of CO analyses obtained by the assimilation of MOPITT V3 CO total column observations with the optimal error estimated by the χ^2 test (top) to the operational MOPITT V3 CO retrieved profiles (middle) at 700 hPa (left panels) and 250 hPa (right panels). The corresponding relative differences between both datasets (TOTCOL_ANALYSES – observations) are indicated in the bottom panels for both pressure levels. Blue and red colors indicate negative and positive differences, respectively. Note that this figure corresponds to an average over August 2008 for all observations carried out over land during daytime.

AMTD
6, 6517–6566, 2013

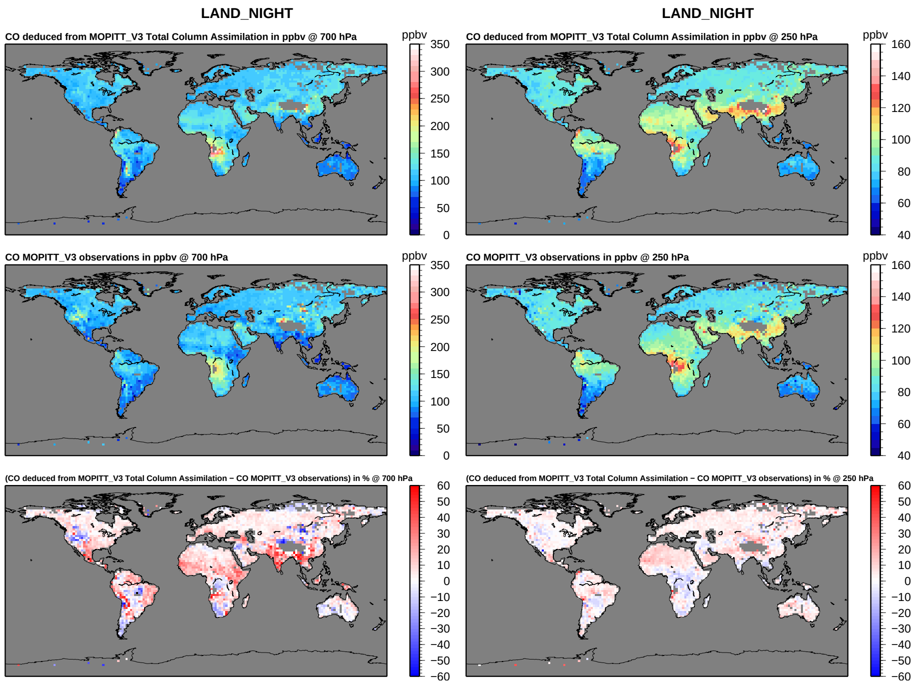

Fig. 6. Same as Fig. 5 but for observations made over land during nighttime (LAND_NIGHT type).

AMTD
6, 6517–6566, 2013

Title Page
Abstract | Introduction
Conclusions | References
Tables | Figures
◂◂ | ▸▸
◂ | ▸
Back | Close
Full Screen / Esc
Printer-friendly Version
Interactive Discussion

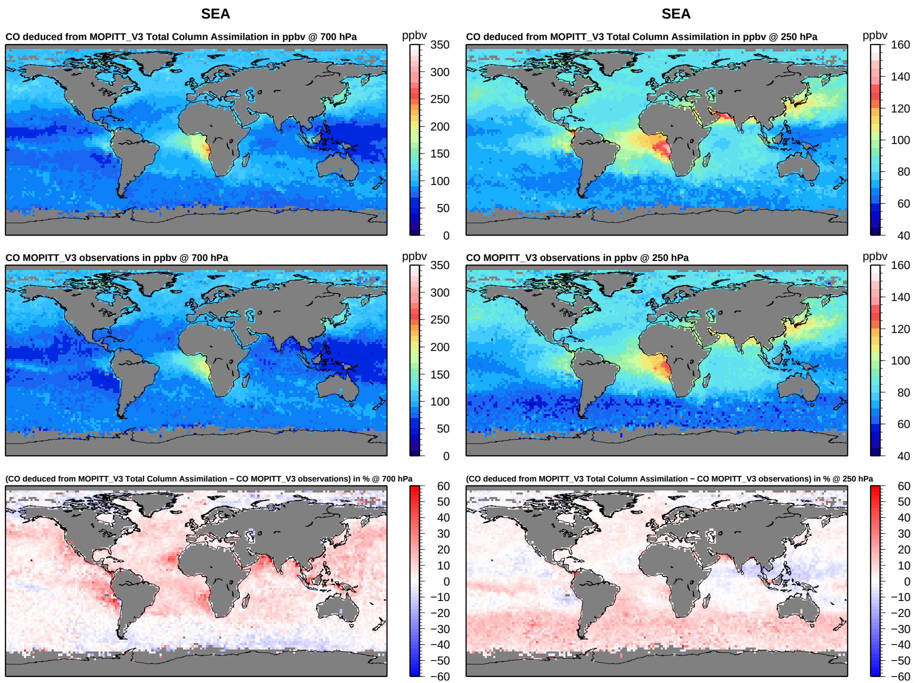

Fig. 7. Same as Fig. 5 but for observations made over sea (SEA type).

AMTD
6, 6517–6566, 2013

CO total column assimilation

L. El Amraoui et al.

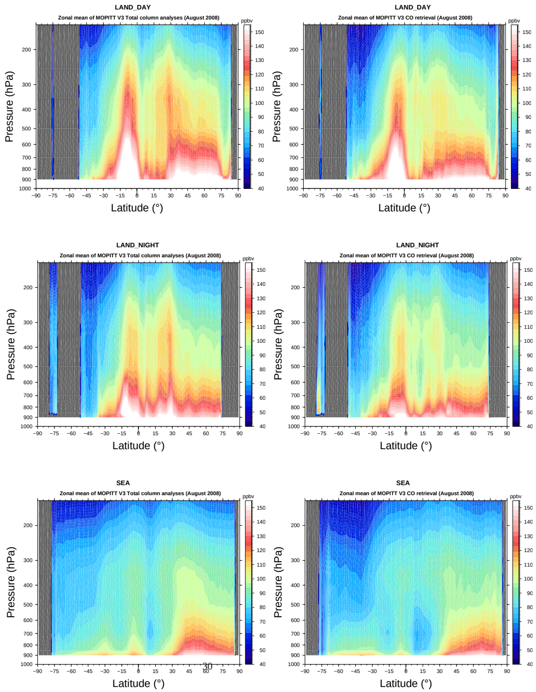

Fig. 8. Zonal mean of MOPITT CO TOTCOL_ANALYSES (left panels) compared to the zonal mean of the MOPITT CO observations (right panels) for August 2008. The comparison is done for observations made: over land during daytime (upper panel), over land during nighttime (middle panel) and over sea during daytime and nighttime (bottom panel).

AMTD
6, 6517–6566, 2013

CO total column assimilation

L. El Amraoui et al.

Title Page
Abstract | Introduction
Conclusions | References
Tables | Figures
◀ | ▶
Back | Close
Full Screen / Esc
Printer-friendly Version
Interactive Discussion

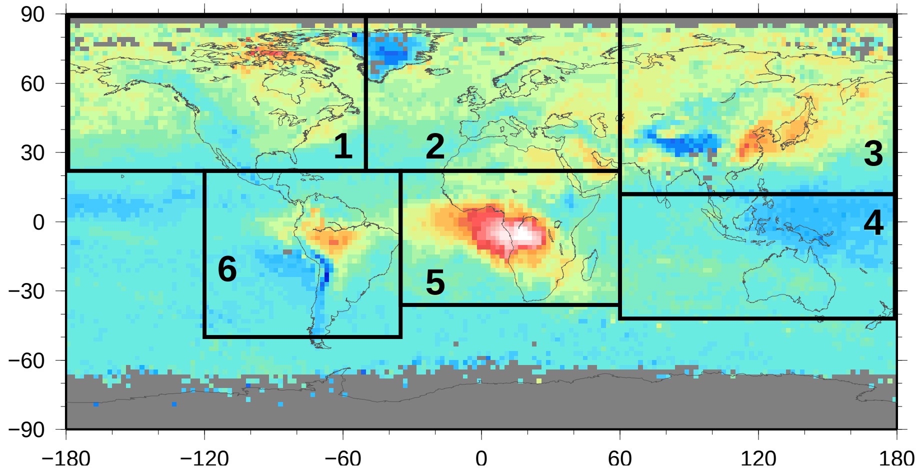

Fig. 9. Main domains of CO emissions considered for the regional validation of the proposed method dealing with the validation of CO TOTCOL_ANALYSES.

AMTD
6, 6517–6566, 2013

CO total column assimilation

L. El Amraoui et al.

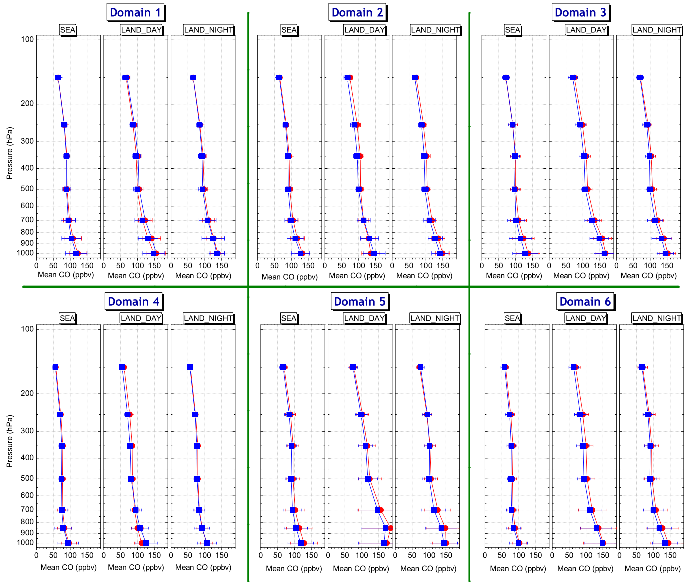

Fig. 10. The mean CO vertical profiles in parts per billion by volume (ppbv) deduced from MOPITT V3 CO TOTCOL_ANALYSES (blue) compared to the operational MOPITT V3 observations (red). Both datasets are averaged over August 2008, over all the domains defined in Fig. 8 and are associated with their corresponding standard deviations.

AMTD

6, 6517–6566, 2013

L. El Amraoui et al.

Title Page
Abstract | Introduction
Conclusions | References
Tables | Figures
Back | Close
Full Screen / Esc
Printer-friendly Version
Interactive Discussion

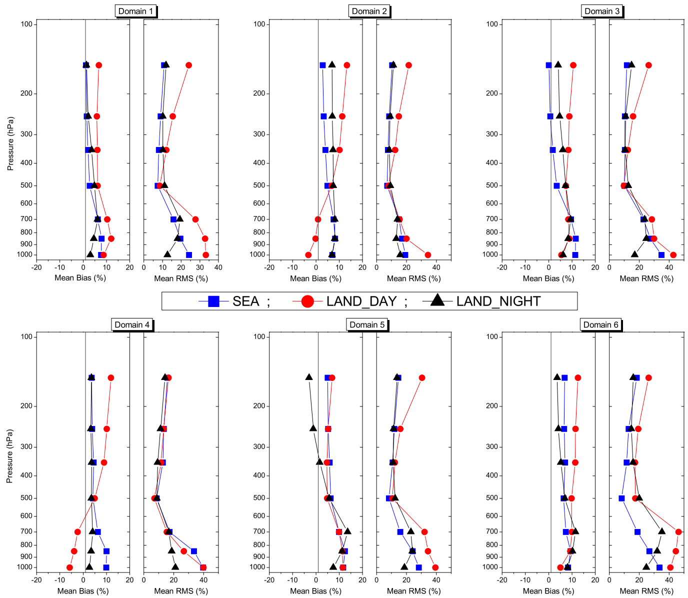

Fig. 11. The mean bias and the corresponding mean RMS (Root Mean Square) between CO vertical profiles deduced from the MOPITT V3 CO TOTCOL_ANALYSES and the MOPITT V3 observations. The comparison is made for observations carried out over land during daytime (red), those carried out over land during nighttime (black) and those carried out over sea (blue).

AMTD
6, 6517–6566, 2013

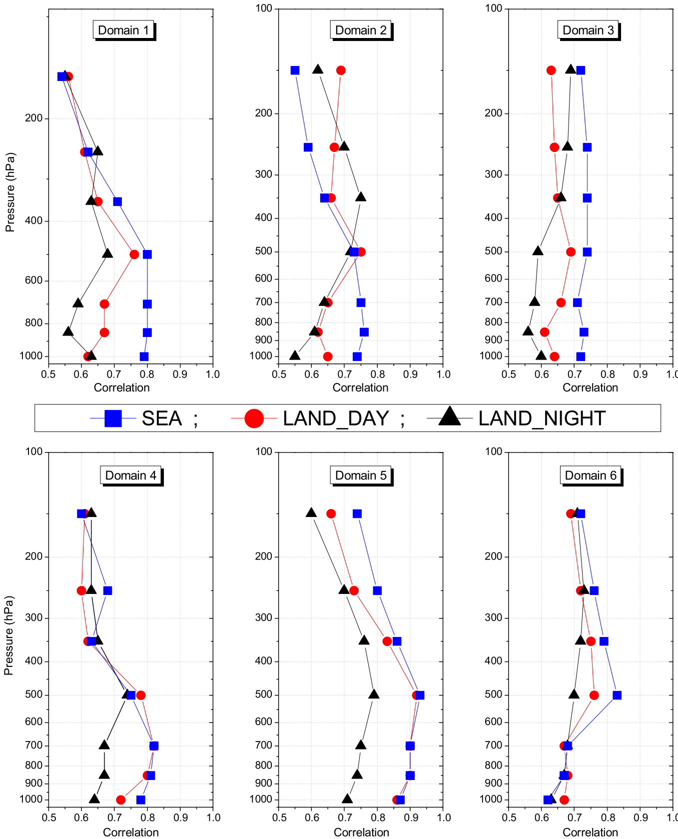

Fig. 12. Same as Fig. 11 but for the correlation coefficient between CO vertical profiles deduced MOPITT CO TOTCOL_ANALYSES and the MOPITT V3 observations. The comparison is made for each level of the MOPITT V3 retrievals.

AMTD
6, 6517–6566, 2013

CO total column assimilation

L. El Amraoui et al.

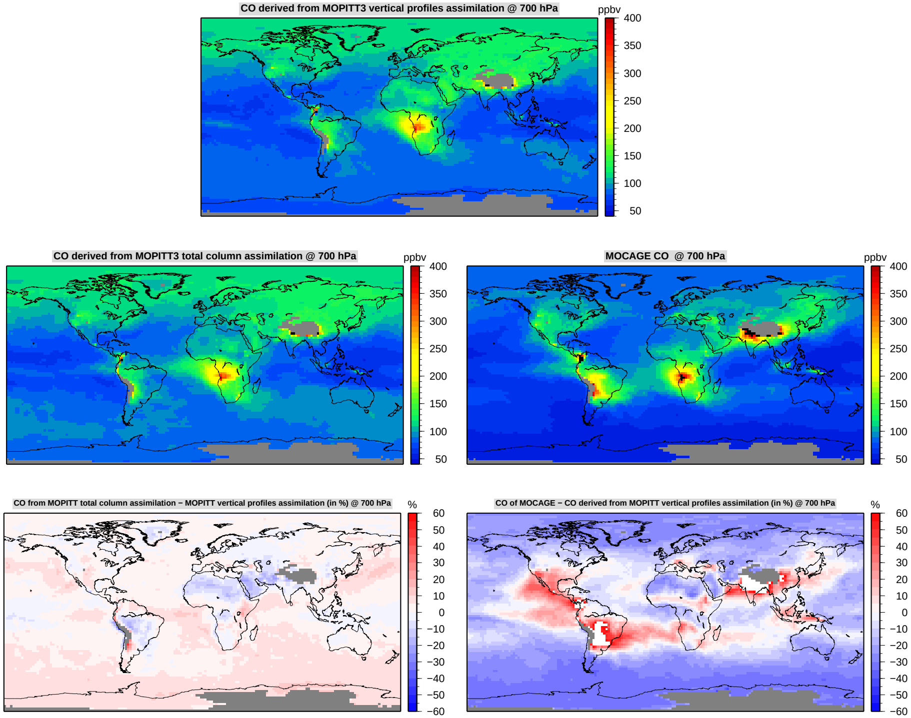

Fig. 13. Maps of CO field at 700 hPa for: (top) MOPITT PROFILE_ANALYSES taking into account averaging kernels and observation error covariance matrices; (middle-left) MOPITT TOTCOL_ANALYSES, and (middle-right) the MOCAGE free-run field. The Figures in the bottom present the difference in % between TOTCOL_ANALYSES and PROFILE_ANALYSES (left), and the difference between the model and PROFILE_ANALYSES (right).

AMTD

6, 6517–6566, 2013

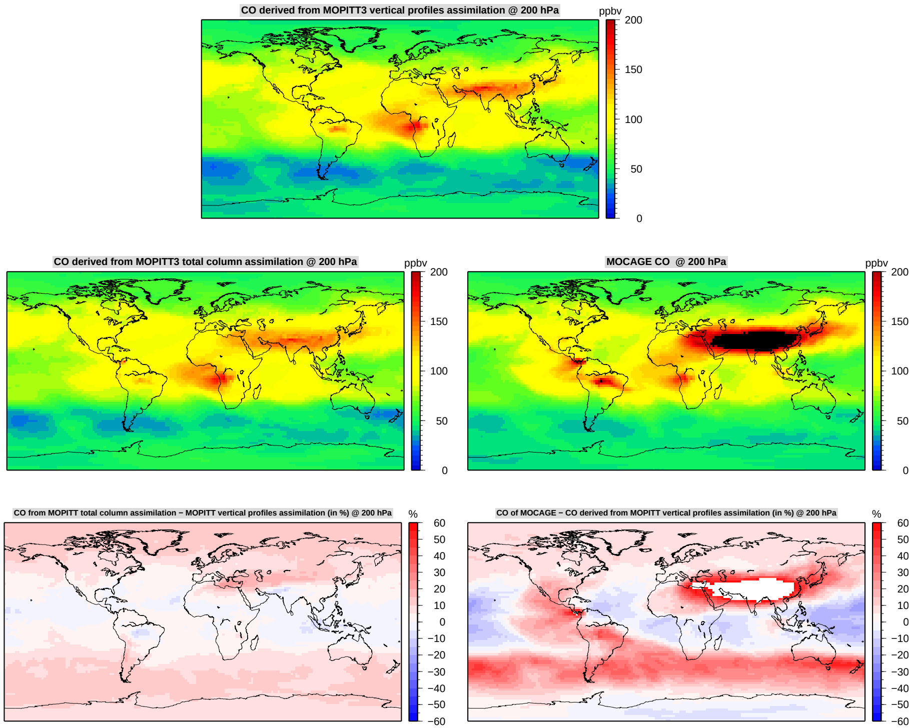

Fig. 14. Same as Fig. 13 but for the pressure level 200 hPa.

AMTD
6, 6517–6566, 2013

CO total column assimilation

L. El Amraoui et al.

Title Page
Abstract | Introduction
Conclusions | References
Tables | Figures
◀| |▶
◀ ▶
Back | Close
Full Screen / Esc
Printer-friendly Version
Interactive Discussion

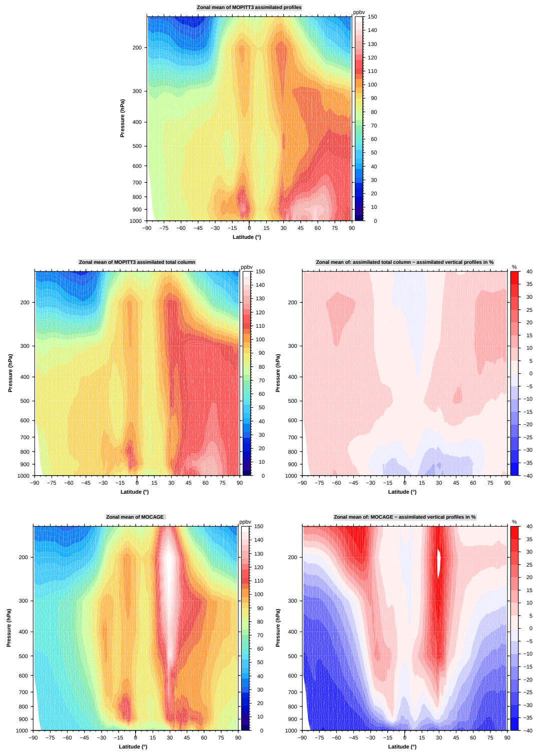

Fig. 15. Zonal means of CO field for the month of August 2008 as obtained by: (top) MOPITT TOTCOL_ANALYSES; (middle-left) MOPITT PROFILE_ANALYSES taking into account averaging kernels and observation error covariance matrices, and (bottom-left) the MOCAGE free-run model. The figures in the right present the difference in % between TOTCOL_ANALYSES and PROFILE_ANALYSES (middle); and the difference between the free-run model and PROFILE_ANALYSES (bottom).

AMTD
6, 6517–6566, 2013

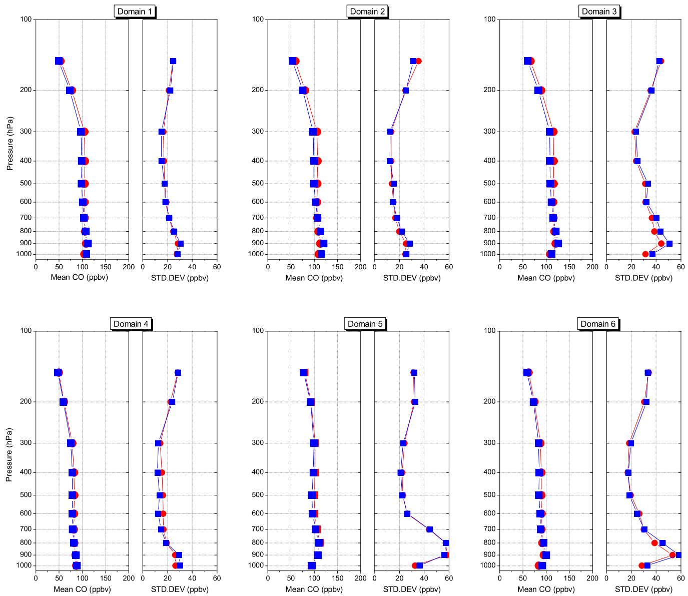

Fig. 16. Mean CO vertical profiles and their associated standard deviations in parts per billion by volume (ppbv) deduced from MOPITT CO TOTCOL_ANALYSES (red) compared MOPITT PROFILE_ANALYSES taking into account the averaging kernels as well as the error covariance matrices (blue). Both datasets are averaged over the month of August 2008 and over all the regional domains defined in Fig. 9.

AMTD
6, 6517–6566, 2013

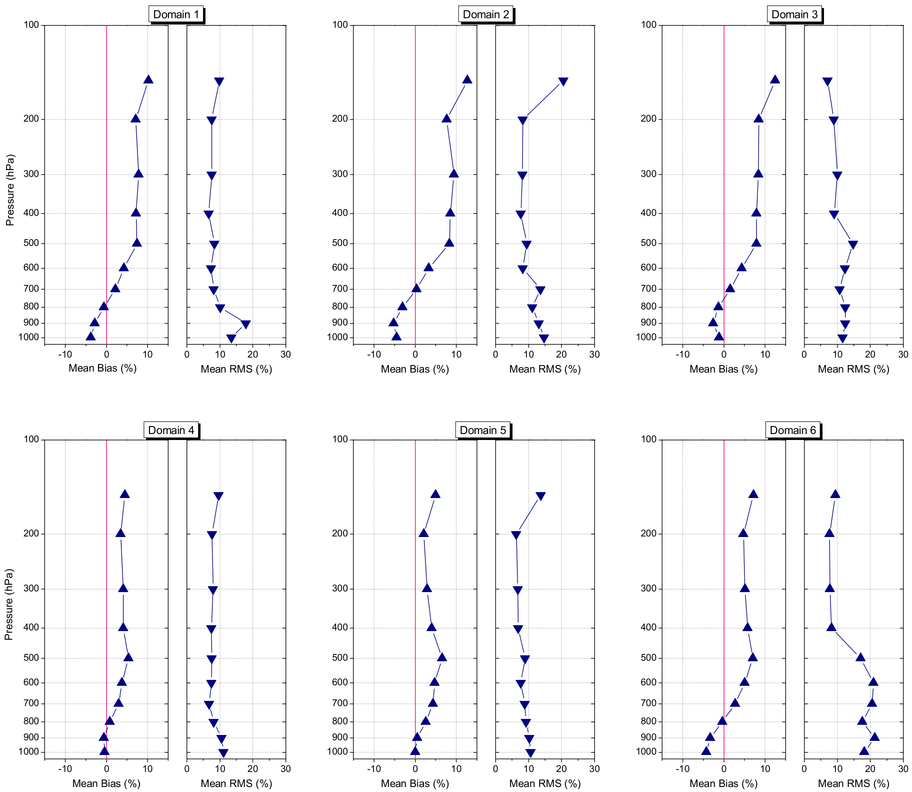

Fig. 17. Same as Fig. 16 but for the mean bias and the corresponding mean RMS (Root Mean Square).

AMTD
6, 6517–6566, 2013

CO total column assimilation

L. El Amraoui et al.

AMTD

6, 6517–6566, 2013

CO total column assimilation

L. El Amraoui et al.

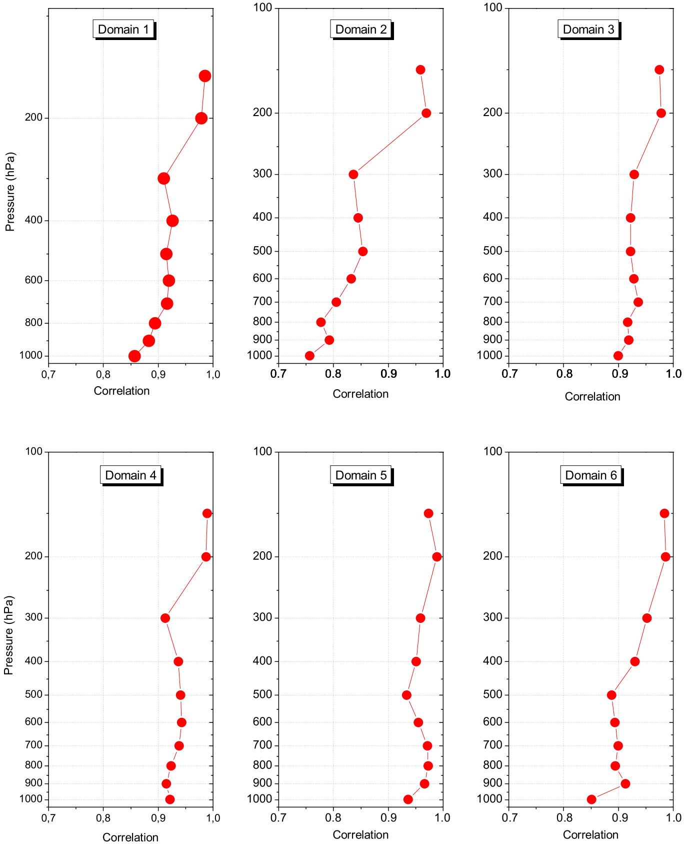

Fig. 18. Same as Fig. 16 but for the correlation coefficient between both analyses (TOT-COL_ANALYSES and PROFILE_ANALYSES).